Preliminary Cone-Ablation Results

KENNETH F. STETSON*
Avco Corporation, Wilmington, Mass.

An approximate analysis is given to permit calculation of nose recession and nose radius of cones during ablation. The results of a preliminary experimental investigation of the ablation of pointed cones give a cursory assessment of cone ablation and an opportunity to check experimental results with the approximate analysis. Six-degree-half-angle cones of Teflon, polyethylene, polystyrene, polyurethane, and ATJ graphite were tested in an air-arc wind tunnel at a Mach number of approximately five. It was found that the pointed cones ablated in a symmetrical, predictable manner and steady-state ablation theory could be used to predict cone ablation. Teflon cones at 10° angle of attack experienced less tip recession but more increase in nose radius than corresponding cones at zero angle of attack. Values for the effective heat of ablation at the stagnation region of the cones were obtained and the data agreed reasonably well with previous results obtained at the stagnation point of stable configurations. The approximate analysis could conveniently be applied to Teflon (a sublimer), and it could give good results. However, it should be used with caution for materials that melt. Estimates of ablated distance and nose radius for an example case of re-entry from a ballistic trajectory are given.

Nomenclature

h_{eff}	=	effective heat of ablation, Btu/lb
h	=	enthalpy, Btu/lb
k	=	const, assumed equal to $q_c(h_{\text{eff}})_{\text{st}}/q_{\text{st}}(h_{\text{eff}})_c$
M	=	Mach number
p	=	pressure, atm
q	=	heat transfer rate, Btu/ft²-sec
R	=	nose radius, ft
RT_0	=	33.86, Btu/lb
t	=	time, sec
T	=	temperature, °R
v	=	velocity, fps
v^*	=	velocity/1000, fps
x	=	ablated distance, ft
dx/dt	=	ablation velocity, fps
W/C_DA	=	ballistic parameter, psf
α	=	angle of attack, deg
β	=	$\frac{1}{24,800}$
γ	=	re-entry angle, deg
θ	=	cone half-angle, deg
θ_H	=	body angle on hemisphere away from stagnation point, deg
ρ	=	atmospheric density, slug/ft³
ρ_M	=	material density, lb/ft³

Subscripts

c	=	cone value
st	=	stagnation value
w	=	value at body surface
e	=	value at the outer edge of the boundary layer

Introduction

ALTHOUGH the pointed-body concept has been known for several years to be a feasible approach† for ablation-type heat shields under high velocity flight conditions, no information has appeared in the literature which would provide a clear understanding of the ablation characteristics of pointed bodies. That is, a wealth of ablation knowledge presently exists; however, such data, for the most part, are associated with stagnation-point ablation. Ablation experiments performed in arc wind tunnels have been with configurations that arrived very early in the test at a stable configuration; thus these experiments produced steady-state ablation data on known configurations. For example, Adams, Powers, and Georgiev[1] found in their experiments that a stable elliptic nose shape with a ratio of major to minor semiaxes of approximately two resulted, regardless of whether the cylinder had an initial hemisphere nose or a flat face. For the case of pointed bodies, a contrasting situation results in which the blunting of the body produces constantly varying heat-transfer rates. Furthermore, it is unlikely for most applications that a stable configuration will be obtained. For example, the nose region of an ablating cone may become a constantly varying parabolic shape during ablation. It is not clearly evident that steady-state ablation analysis can be applied directly to such ablation conditions.

Without a better understanding of the ablation characteristics of pointed bodies, it is difficult to make meaningful predictions of such critical factors as cone-point recession and nose radius. The cone-point recession and the associated nose radius are required in order to estimate boundary-layer phenomena and heat-shield requirements.

The purpose of the arc wind-tunnel experiments described herein was to take a preliminary look at the ablation characteristics of pointed cones and to examine the capability of an approximate analysis for predicting cone recession and nose radius. Several materials were selected which may have application to future pointed vehicle configurations.

Experimental Techniques

The experiments were performed in a 10-Mw air-stabilized arc wind tunnel (Fig. 1) described by Bond et al.[2] This facility has four radially mounted arcs exhausting into a single plenum chamber. The nozzle comprises a 7° half-angle cone matched to a contoured section to give 1-ft diam for a nominal Mach 5 test section. Blowdown runs last up to 60 sec. As often happens with new facilities, the present experiments were performed in the tunnel before a complete calibration had been accomplished; indeed, a facility of this type probably never will be calibrated with the same degree of accuracy and reliability obtained with more conventional wind tunnels. However, an attempt was made to perform all of the experi-

Presented as Preprint 64-433 at the 1st AIAA Annual Meeting, Washington, D. C., June 29–July 2, 1964; revision received December 23, 1964. This work was sponsored by the Air Force Ballistic Systems Division, Air Force Systems Command, U. S. Air Force under Contract No. AF04(694)-239. The author gratefully acknowledges the assistance of many associates at Avco/RAD, in particular, D. Lang for his assistance with the data reduction and W. Kukers for obtaining the models. Thanks go to members of the Aerodynamics Section for conducting the experiments, especially A. Todisco and R. Freeman.

* Senior Project Engineer. Member AIAA.

† For example, this point was emphasized by Detra and Kantrowitz in an unpublished Avco note in 1959 after performing some exploratory ablation experiments with pointed cones.

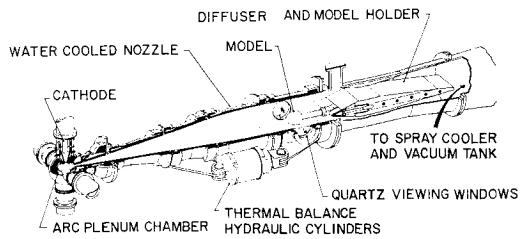

Fig. 1 Cutaway of hyperthermal wind tunnel.

ments with the following test section conditions: $h_{st}/RT_0 = 200$, $p_{st} = 0.3$ atm (pitot pressure), $M = 5$. Several calibration runs with pressure rakes and calorimeter models verified the stagnation pressure of 0.3 atm in the test section and indicated that a value of $qR^{1/2}$ of 180 Btu-ft$^{1/2}$/ft^2-sec was obtained. (By utilizing available calibration data[2] for other test conditions, it was possible to estimate the change in test conditions resulting from variations from run to run.) These conditions result in stagnation-point conditions on the model corresponding to those for a flight velocity of 18,300 fps at an altitude of 165,000 ft. Mach number effects, of course, are not matched, and they may be significant for pointed configurations and particularly for ablation materials that melt and flow, such as polyethylene, polystyrene, and polyurethane.

The combination of low density and small nose radius associated with these experiments places the cone tip in a flow regime where transport effects immediately behind the shock- and vorticity-interaction effects may increase the stagnation-point heat-transfer rates over those predicted by "conventional" boundary-layer theory, e.g., Fay and Riddell.[3] For a typical test, the Reynolds number based on stagnation-point conditions and the nose radius ($Re = \rho_{st}Rh_{st}^{1/2}/\mu_{st}$) varied from about 135 after 1 sec of testing to about 1350 after 20 sec. The calibration models (used to obtain the value of $qR^{1/2} = 180$) had a corresponding Reynolds number of approximately 3000 ($R \cong 0.25$ in.). The heat-transfer rates obtained from these calibrations were approximately 15% higher[2] than the calculated values obtained by using the theory of Fay and Riddell.[3] It is not meant to imply that this difference can be entirely accounted for by low-density effects, but such an increase is compatible with theories of Ferri and Zakkay[4] and Cheng.[5] Throughout the Reynolds number range of the cone experiments and the calibration tests, the increased stagnation heating due to low-density effects was approximately the same (according to Refs. 4 and 5), making it unnecessary to take into account the differences in Reynolds number between the calibration models and the models being tested.

The models used for these experiments were 6° half-angle cones with a 2-in. base diameter, made from Teflon, polyethylene, polystyrene, polyurethane, and ATJ graphite. Figure 2 shows photographs of a typical polyethylene model before and after test. The polystyrene model had a slightly ogival tip; hence the results for this test should not be compared directly with the rest of the data. Three of the polyethylene models were irradiated by a 2-Mev Van de Graa accelerator‡ to produce a cross-linking of the polymer chains and thereby suppress flowing during ablation. The models were placed on their sides and given a dosage of 15×10^6 rad,§ then rotated 180° and given the same dosage on the other side. Two of the three irradiated models had the first inch of the cone behind the tip completely shielded, so that no cross-linking of that area resulted. This technique provided a means of comparing the ablation characteristics of "regular"

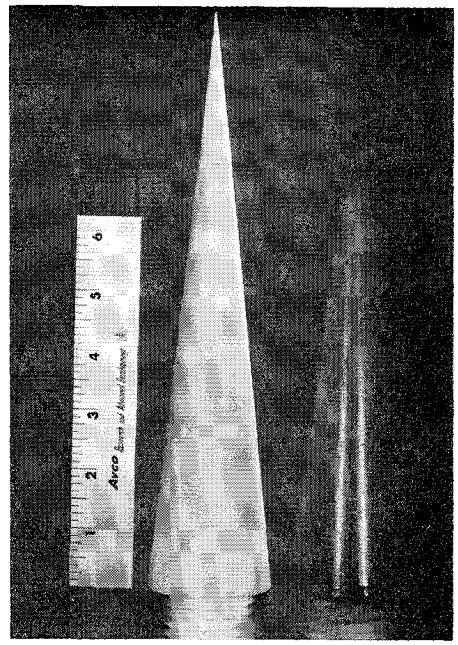

Fig. 2 Polyethylene model before and after 20-sec test.

and irradiated polyethylene during a single test, and thus avoided some of the uncertainty that results from comparisons made from two supposedly identical tests.

The tip recession and the change in nose radius were obtained from enlargements of 16-mm movies taken at 24 frames/sec. Figure 3 shows representative enlargements from the films for a polyethylene cone $\alpha = 0$ and a Teflon cone at $\alpha = 10°$. The top photo was the first frame in which flow over the model was observed ($t = 0$), and succeeding frames represent 5-sec intervals. The boundary layers, which contain the products of ablation, radiate intensely in the visible wavelength region so that they are clearly visible during the test, particularly on the leeward side of the Teflon model. The graphite model (not shown) ablated only a

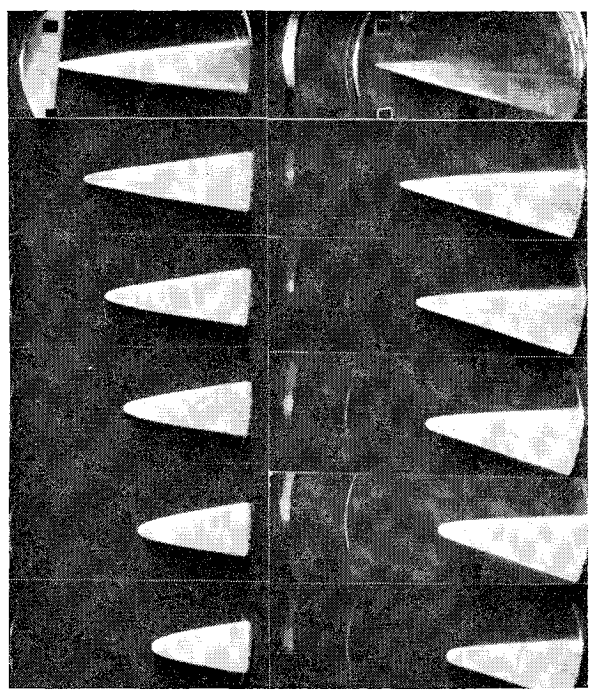

Polyethylene, $\alpha = 0$ Teflon, $\alpha = 10°$

Fig. 3 Representative frames (5-sec intervals, beginning at $t = 0$ at top) from motion pictures of ablation tests.

‡ Models were irradiated at High Voltage Engineering Corporation, Burlington, Mass.

§ Rad is a measurement of absorbed radiation equal to 100 erg/g. One million rad equals 4.5 kw-sec/lb.

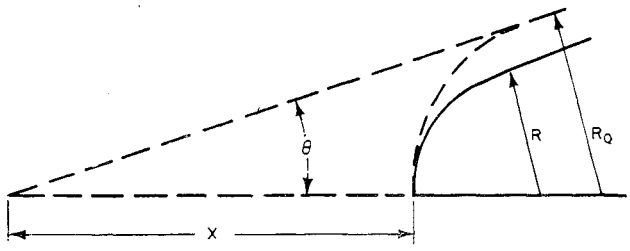

Fig. 4 Sketch of cone tip.

small amount (and, of course had different products of ablation) and did not produce a visible boundary layer.

Results

For the most part, ablation theory and experiment have been concerned with steady-state ablation conditions, resulting from constant heat-transfer rates on stable configurations. New problems are introduced with cone ablation, since the cone tip dimensions, and hence the heat-transfer rates, are constantly changing. This paper has assumed that, for the case of cones exposed to high heat-fluxes, a quasi-steady-state ablation situation existed and that conventional steady-state ablation concepts could be applied.

Therefore, the energy absorbed per unit mass, or the effective heat of ablation h_{eff}, is defined as the aerodynamic heat-transfer rate to a nonablating surface (at the ablation temperature) divided by the rate of mass loss:

$$h_{eff} = q/(\rho_M dx/dt) \tag{1}$$

or

$$R^{1/2}dx/dt = q_{st}R^{1/2}/(h_{eff})_{st}\rho_M \tag{2}$$

In order to integrate Eq. (2) to obtain a relationship for tip recession, it was necessary to express the nose radius (R) in terms of the ablated distance (x). From Fig. 4 it can be seen that, for the case of no mass loss from the sides of the cone, this relationship was simply

$$R_0 = x \sin\theta/(1 - \sin\theta) \tag{3}$$

In order to apply a correction to Eq. (3) to account approximately for the effects of surface recession along the cone, several approximations were made. It was assumed that 1) steady-state ablation analyses could be applied to ablation on the side of the cone as well as in the stagnation region, 2) the boundary layer was laminar, and 3) q_c/q_{st} and $(h_{eff})_{st}/(h_{eff})_c$ were not time-dependent.

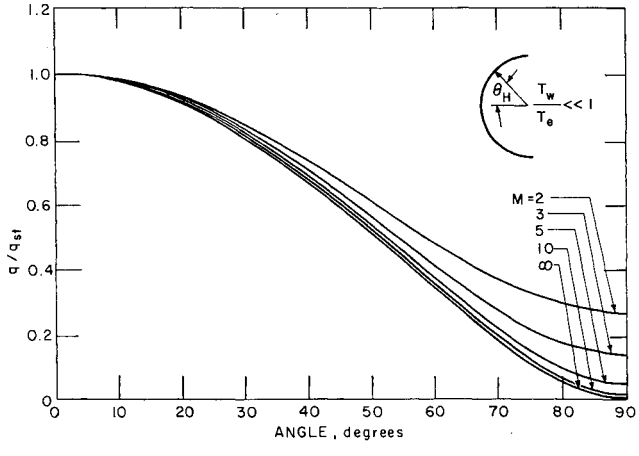

Fig. 5 Laminar heat-transfer rate distribution over isothermal hemisphere nose (from Ref. 6).

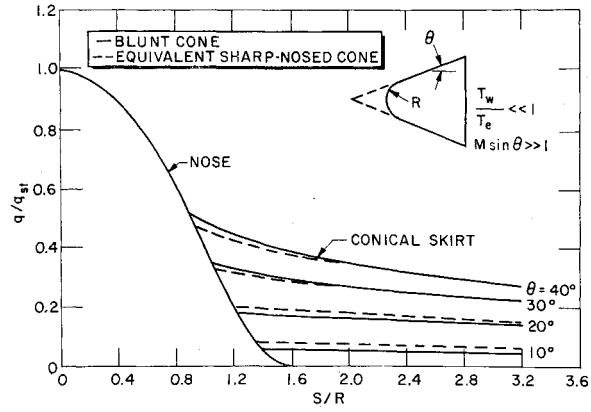

Fig. 6 Laminar heat-transfer rate distribution over blunt cones (from Ref. 6).

As will be shown later, an examination of the data indicated that steady-state ablation analyses could be applied to the stagnation region from the start of the test (i.e., $x \propto t^{2/3}$). The surface recession history along the side of the cones included the combined effects of any unsteady ablation, changes in the effective heat of ablation, and changes in the heat-transfer rate; and it was not possible to accurately separate these effects. However, by comparing the data from the melting plastic cones with that obtained from the Teflon cones [which should be the best example of constant $(h_{eff})_c$] it appeared that the departure of the data from predictions for the melting cones was dominated by changes in $(h_{eff})_c$. This point will be discussed in more detail later. An appropriate value for q_c/q_{st} was obtained from laminar heat-transfer data on blunted cones.[6] Figures 5 and 6, which contain results from Ref. 6, are shown for convenience. Estimating $(h_{eff})_{st}/(h_{eff})_c$ will, in general, be more difficult to determine since $(h_{eff})_c$ will probably be unknown for most materials. For the calculations of this paper, this ratio of the effective heats of ablation has been assumed equal to unity. This is probably a reasonable assumption for a subliming material, such as Teflon, but it may introduce significant error for materials that melt.

From Eq. (2), and subsequently Eq. (7), it can be seen that $xt \propto {}^{2/3}$. Since q_c/q_{st} has been assumed constant, then $q_c \propto R^{-1/2}$ and the expression for cone surface recession $(R_0 - R)$ resembles Eq. (2) and also becomes proportional to $t^{2/3}$. Then

$$\frac{\text{cone surface recession}}{x} = \frac{R_0 - R}{x} \cong \frac{(h_{eff})_{st}q_c}{(h_{eff})_c q_{st}} \cong k \tag{4}$$

Combining Eqs. (3) and (4) results in

$$R \cong \{[\sin\theta/(1 - \sin\theta)] - k\}x \tag{5}$$

Substitution of Eq. (5) into Eq. (2) gives

$$\left(\frac{\sin\theta}{1 - \sin\theta} - k\right)^{1/2} \int_{x_1}^{x_2} x^{1/2}dx \cong \frac{q_{st}R^{1/2}}{(h_{eff})_{st}\rho_M} \int_{t_1}^{t_2} dt \tag{6}$$

and integration results in

$$x_2 \cong \left[\left(\frac{3}{2}\frac{q_{st}R^{1/2}}{(h_{eff})_{st}\rho_M}\right)\frac{t_2 - t_1}{\{[\sin\theta/(1 - \sin\theta)] - k\}^{1/2}} + x_1^{3/2}\right]^{2/3} \tag{7}$$

Equation (7) can be used to predict ablation distances in arc wind-tunnel experiments since $qR^{1/2}$ is a constant during a test. Note that this expression (and subsequent ones) fails as $[\sin\theta/(1 - \sin\theta)] \to k$. This implies that $R \to 0$, or $q_{st} \to \infty$. As this condition is approached, blunting would probably cease and the cone remain essentially pointed during ablation. Such a situation might occur, for instance, when

the Mach number is low,¶ turbulent boundary layers exist on the sides of the cone, or the material properties are such that h_{eff} on the sides of the cone is less than at the stagnation region.

If one wants to estimate ablated distance in the flight case, for example, a vehicle re-entering the atmosphere, where $qR^{1/2}$ is constantly varying, the following approach may be used. Lees[7] gave the following approximate relationship:

$$q_{st}R^{1/2} \cong 21.9\rho^{1/2}v^{*3} \tag{8}$$

Substitution in Eq. (6), now considering $qR^{1/2}$ and h_{eff} as variables, gives

$$\left(\frac{\sin\theta}{1-\sin\theta}-k\right)^{1/2}\int_{x_1}^{x_2}x^{1/2}\,dx \cong \frac{21.9}{\rho_M}\int_{t_1}^{t_2}\frac{\rho^{1/2}v^{*3}}{(h_{\text{eff}})_{st}}\,dt \tag{9}$$

Since this analysis is only meant to give approximate results, no attempt will be made at this time to consider velocity and the effective heat of ablation as variables. A simple example will be considered, i.e., that of early re-entry of a high velocity re-entry vehicle. For a high performance re-entry vehicle (high W/C_DA) it is probably reasonable to assume (for these purposes) that the vehicle velocity is constant and the boundary layer at the tip is laminar down to 100,000 ft. Also, many low-temperature ablating materials have an effective heat of ablation which is essentially constant down to this altitude. In order to change the variable of integration from dt to $d\rho$, the following relationships given by Allen and Eggers[8] are utilized:

$$dy/dt = -v\sin\gamma \tag{10}$$

$$\rho = \rho_0 Ce^{-\beta y} \tag{11}$$

$$d\rho/dy = -\beta\rho_0 Ce^{-\beta y} = -\beta\rho \tag{12}$$

$$dt = d\rho(d\rho/dy)^{-1}(dy/dt)^{-1} \tag{13}$$

Therefore,

$$dt = d\rho/(\beta\rho v\sin\gamma) \tag{14}$$

Substitution in Eq. (9) results in

$$\left(\frac{\sin\theta}{1-\sin\theta}-k\right)^{1/2}\int_{x_1}^{x_2}x^{1/2}\,dx \cong \frac{0.0219\,v^{*2}}{\rho_M(h_{\text{eff}})_{st}\,\beta\sin\gamma}\int_{\rho_1}^{\rho_2}\rho^{-1/2}d\rho \tag{15}$$

Integration and solution for x_2 gives

$$x_2 \cong \left[\left(\frac{0.066\,v^{*2}}{\rho_M(h_{\text{eff}})_{st}\,\beta\sin\gamma}\right)\times\frac{(\rho_2^{1/2}-\rho_1^{1/2})}{\{[\sin\theta/(1-\sin\theta)]-k\}^{1/2}}+x_1^{3/2}\right]^{2/3} \tag{16}$$

The nose radius at any altitude can be estimated in a similar manner. From Eq. (5) can be obtained

$$dR = \{[\sin\theta/(1-\sin\theta)]-k\}dx \tag{17}$$

and substitution in Eq. (2) results in

$$\frac{R^{1/2}dR}{\{[\sin\theta/(1-\sin\theta)]-k\}} = \frac{q_{st}R^{1/2}}{(h_{\text{eff}})_{st}\rho_M}\,dt \tag{18}$$

and integration gives

$$R_2 \cong \left[\left(\frac{0.066v^{*2}}{\rho_M(h_{\text{eff}})_{st}\beta\sin\gamma}\right)\left(\frac{\sin\theta}{1-\sin\theta}-k\right)\times(\rho_2^{1/2}-\rho_1^{1/2})+R_1^{3/2}\right]^{2/3} \tag{19}$$

¶ Many facilities used for ablation tests have $M < 3$. Care should be exercised when interpreting cone blunting data obtained from such facilities, since, due to the low M, they may indicate very little blunting.

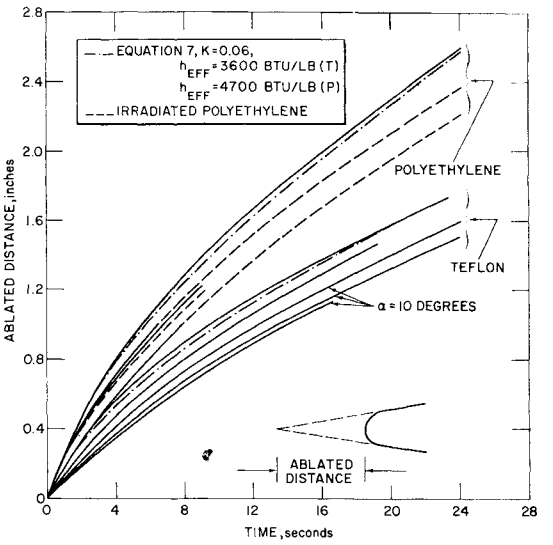

Fig. 7 Ablation curves for Teflon and polyethylene; $h_{st}/RT_0 \cong 200$, $p_{st} \cong 0.3$ atm, $qR^{1/2} \cong 180$ Btu (ft)$^{1/2}$/ft^2-sec.

For arc wind-tunnel experiments, where $qR^{1/2}$ is a constant during a test, Eq. (18) can be easily integrated to predict the nose radius to be obtained at any time during a test:

$$R_2^{3/2} - R_1^{3/2} \cong \frac{3}{2}\left(\frac{\sin\theta}{1-\sin\theta}-k\right)\left(\frac{q_{st}R^{1/2}}{(h_{\text{eff}})_{st}\rho_M}\right)(t_2-t_1) \tag{20}$$

and for the case of a sharp point, at the beginning of the test $R_1 \cong 0$ when $t_1 = 0$, and

$$R \cong \left[\frac{3}{2}\left(\frac{\sin\theta}{1-\sin\theta}-k\right)\left(\frac{q_{st}R^{1/2}}{(h_{\text{eff}})_{st}\rho_M}\right)t\right]^{2/3} \tag{21}$$

Figure 7 contains experimental ablation results for several Teflon and polyethylene cones. Previous experiments with blunt cylinder configurations found the ablated distance to be linearly related to test time (after steady-state ablation conditions were realized). Equation (7) indicates that, for cone ablation, the ablated distance is proportional to $t^{2/3}$, or a semi-cubic parabola. The experimental data were found to follow such a curve very closely. That is, for the tunnel test conditions that gave values of $h_{st}/RT_0 \cong 200$ and $p_{st} \cong 0.3$ atm, $qR^{1/2}$ was found from the tunnel calibrations to be approximately 180. Using available information, the effective heat of ablation of Teflon at the stagnation point was taken at 3600 Btu/lb (see, e.g., Ref. 9) and for polyethylene $(h_{\text{eff}})_{st}$ was assumed to be 4700 Btu/lb. Substitution of these values into Eq. (7) gave a reasonable prediction of the experimental results obtained for zero angle of attack. The ablated distances for the Teflon cones at $\alpha = 10°$, at any given time, were always less than the ablated distances for $\alpha = 0$. The cone ablation at angle of attack was not symmetrical, and the resulting nose radius was greater than the corresponding cone at $\alpha = 0$ (see Fig. 8). If the models were spinning, this result probably would not have occurred. The two irradiated polyethylene models with the first inch of the tip shielded are shown with a solid line for the first inch of ablation and then a dashed line for the remainder of the test. There does not appear, from the results shown on this figure, to be any noticeable improvement in the ablation characteristics of the cross-linked polyethylene; however, this point will be discussed in more detail later.

It is of interest to note that the starting transient for the ablation of blunt cylinders[1] lasted from 10–25 sec. (As observed on a plot of ablated distance vs test time, this was the time when the slope of the curve became constant.) A corresponding starting transient was not observed for these cone ablation experiments in that the ablated distance was

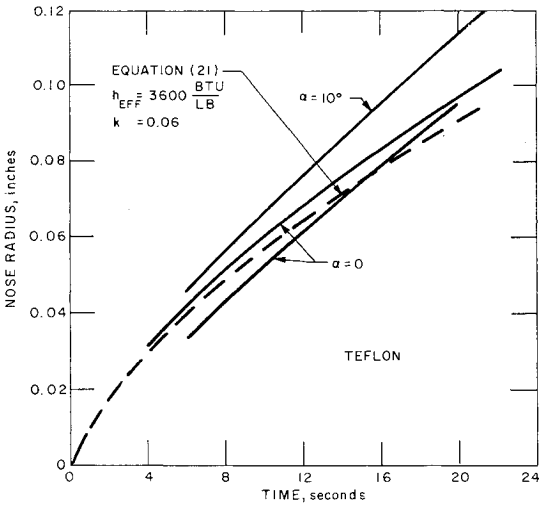

Fig. 8 Nose-radius curves for Teflon; $h_{st}/RT_0 \cong 200$, $p_{st} \cong 0.3$ atm, $qR^{1/2} \cong 180$ Btu (ft)$^{1/2}$/ft^2-sec.

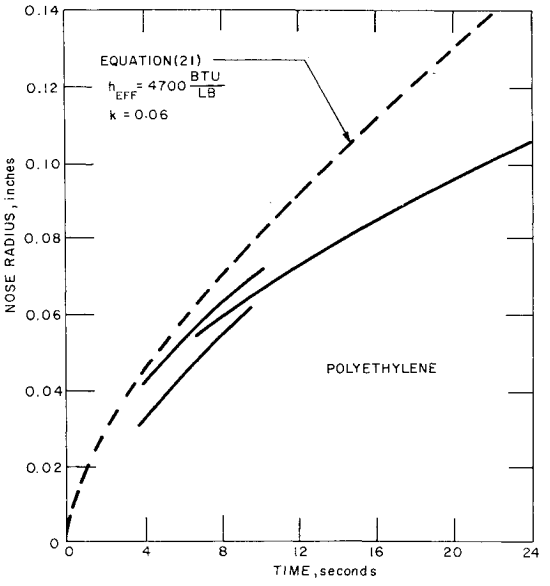

Fig. 10 Nose-radius curves for polyethylene; $h_{st}/RT_0 \cong 200$, $p_{st} \cong 0.3$ atm, $qR^{1/2} \cong 180$ Btu (ft)$^{1/2}$ft^2-sec.

proportional to $t^{2/3}$ from the start of the test. Since the $t^{2/3}$ proportionality was based on steady-state analyses, these results imply quasi-steady ablation with negligible starting transients.

Figure 9 contains the results from single tests with polyurethane, polystyrene, and ATJ graphite models. Since the polystyrene model resembled an ogive in the tip region, it was expected that the tip recession rate would be less than predicted from cone theory. The graphite model had only a small loss of material as can be seen by the small ablated distance of the tip. The graphite cone behaved essentially as a heat sink with the tip quickly heating until the surface glowed. As the test progressed, the glowing region proceeded rearward on the cone until the entire cone was glowing at the end of the test.

Figure 8 compares nose radii for the Teflon cones. For $\alpha = 0$, the differences between the data and the values predicted by Eq. (21) are within the reading error of the nose radius measurements. The nose radii for the cones at $\alpha =$ 10° were all nearly the same; thus only one curve is shown which represents an average of the three tests. The ablation was not symmetrical for the cones at angle of attack, and the nose radius, at any given time, was greater than the corresponding cones at zero angle of attack. The fact that Eq. (21), with its associated assumptions, predicted well the nose radius history of the Teflon cones implies that the ablation was quasi-steady and $(h_{cff})_{st}q_c/(h_{cff})_c q_{st} \cong$ const.

Figure 10 shows that for polyethylene cones Eq. (21) overestimated the nose radius. Since the Teflon experiments have established the validity of the quasi-steady ablation assumption for these tests, it appears that the departure from predictions for the polyethylene cones was dominated by changes in $(h_{eff})_c$. The error introduced by the assumption of $(h_{eff})_{st}/(h_{eff})_c = 1$ for melting plastics will perhaps be more clearly evident from data contained in Fig. 11.

Figure 12 shows typical cone contours at selected test times. In some instances, the radiating boundary layer obscured the cone surface to such an extent that cone tip dimensions were difficult to obtain. However, dimensions taken from the model after the test agreed well with the corresponding dimensions obtained at the termination of the film record, and so it was concluded that the contours shown are a fairly good representation of the actual contours. The re-

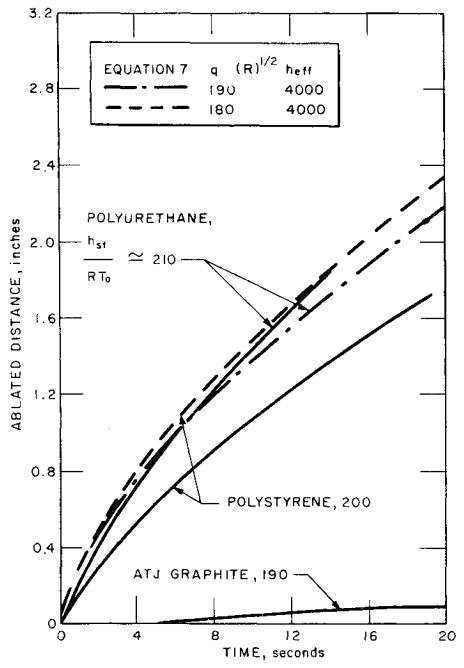

Fig. 9 Ablation curves for polyurethane, polystyrene, and ATJ graphite.

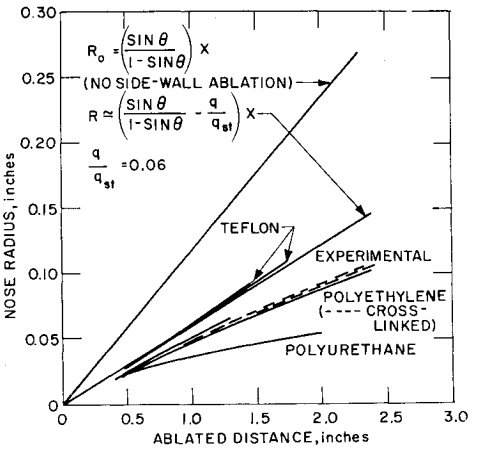

Fig. 11 Nose-radius vs ablated distance; $M \cong 5$, $h_{st}/RT_0 \cong 200$, $p_{st} \cong 0.3$ atm.

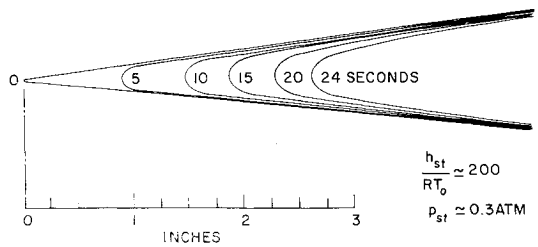

Fig. 12. Polyethylene cone contours.

sults of ablation on the sides of the cone cause the tip region of the cone to change from a conical shape to a parabolic shape. Polyurethane maintained a small nose radius even though the tip had ablated nearly 2 in. It appears that by proper choice of material, cone angle, or test conditions, it would be possible to achieve a stable nose shape that would remain unchanged after the initial few seconds of exposure.

In order to accurately predict the cone tip recession and the nose radius during ablation, it is necessary to know the relationship between nose radius and cone tip recession. Figure 11 shows this relationship for the Teflon, polyethylene and polyurethane cones tested in these arc tunnel experiments. It can be seen that the nose radius of the Teflon cones can be represented simply as

$$R \cong \{[\sin\theta/(1 - \sin\theta)] - q/q_{st}\}\, x$$

As mentioned previously, it was expected that such a relationship would be reasonable for a subliming material. (However, the close agreement shown for Teflon is perhaps fortuitous and should not be interpreted as being indicative of the accuracy to be expected for subliming materials.) The polyethylene and polyurethane cones show the deviation that can occur with materials that melt. There does not appear to be a simple way of writing a general expression to show the relationship between nose radius and tip recession for melting materials. That is, the dependence upon such things as cone angle, boundary-layer conditions, heating rates, and shear stresses are not known in sufficient detail at this time.

If one properly related the dependence of the nose radius upon tip recession, then values of h_{eff} obtained from these cone ablation experiments should be compatible with data obtained from other configurations. In order to check this point, Eq. (6) was integrated and solved for $(h_{eff})_{st}$

$$(h_{eff})_{st} \cong \frac{3}{2} \frac{q_{st}R^{1/2}}{\rho_M \{[\sin\theta/(1 - \sin\theta)] - k\}^{1/2}} \frac{t_2 - t_1}{x_2^{3/2} - x_1^{3/2}} \quad (22)$$

where x is in feet.

The ablated distance (x) was taken from the motion picture records, $q_{st}R^{1/2}$ from the calibrations, and $\{[\sin\theta/(1 - \sin\theta)] - k\}$ from Fig. 11. The results are presented in Figs. 13 and 14 and the agreement with previous data is considered reasonable. Figure 13 contains data from both "regular" and cross-linked polyethylene. It was felt that the cross-linking of the polyethylene polymer chain might inhibit the melting and improve its cone ablation characteristics. However, from the few experiments performed, there would have to be a significant effect in order to separate it confidently from the normal experimental scatter. Even though Fig. 13 indicates a higher effective heat of ablation at the stagnation region for the irradiated models, the results are felt to be inconclusive. If the cross-linking had much effect in restricting melting, the results would probably be more noticeable on the sides of the cone than at the stagnation region, due to the lower heating rates and higher shear forces

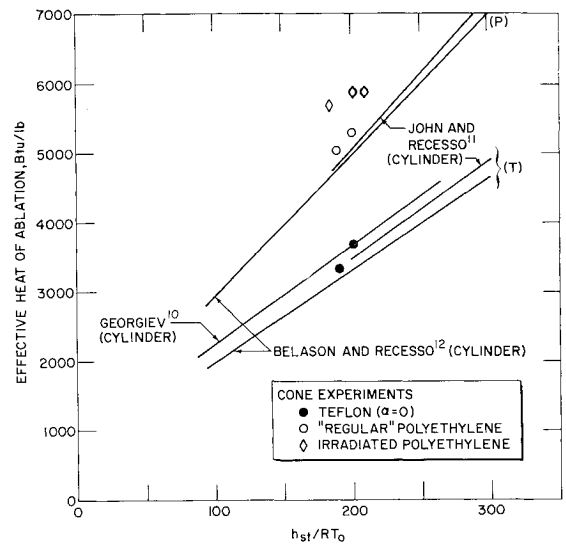

Fig. 13 Effective heat of ablation for Teflon and polyethylene.

on the sides of the cone. This would result in a difference in the relationship between x and R. With this reasoning, Fig. 11 should be consulted as well as Figs. 13 and 7. However, inspection of Fig. 11 shows a randomness of the data typical of experimental scatter and no significant differences are observed between the irradiated and the nonirradiated models. The conclusion was then made, utilizing data from Figs. 7, 11, and 13, that there was no significant improvement in the ablation characteristics of the polyethylene cones by the cross-linking of the polymer chains.

Equations (16) and (19) have been utilized to estimate ablated distance and nose blunting for a flight example. The results for a Teflon cone, with cone angle as a parameter, are shown in Figs. 15 and 16. The curves are shown as broken lines below 100,000 ft, since the assumptions of constant velocity and h_{eff} become less valid. However, since these deviations have a compensating effect, "exact" calculations between 100,000 and 50,000 ft would not differ greatly from the values shown. These results indicate that small nose radii may be maintained on a cone to altitudes below 100,000 ft for typical high-velocity re-entries. When the boundary layer on the cone goes through transition from laminar to turbulent, the nose configuration may enter into a different type of configuration change, and it is conceivable, for some situations that the nose radius may get smaller. That is, the higher heating rates and lower values of effective heat of ablation associated with a turbulent boundary layer would result in greater mass loss than for the regions of the cone covered with a laminar boundary layer. For these

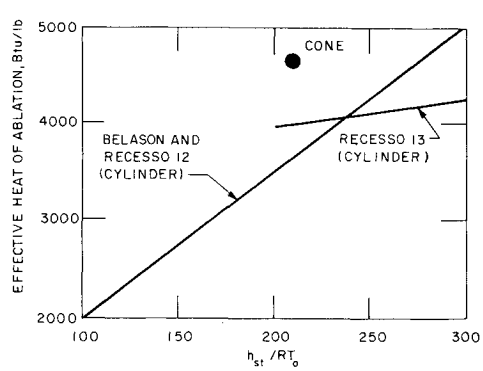

Fig. 14 Effective heat of ablation for polyurethane.

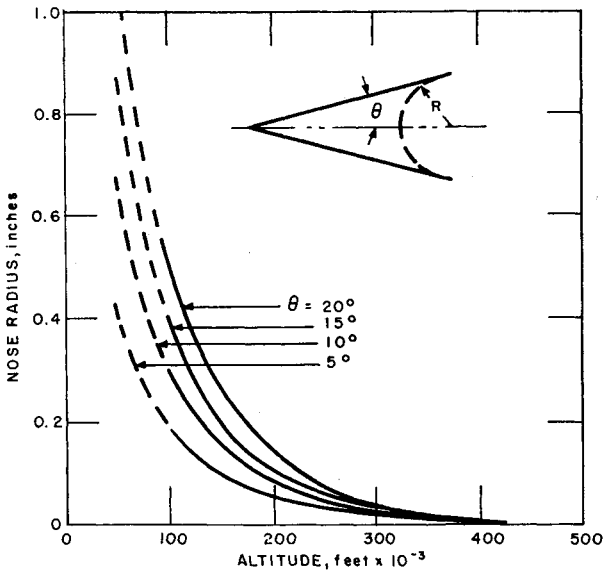

Fig. 15 Nose-radius vs altitude for Teflon; v = 24,000 fps, γ = 20°, h_{eff} = 5000 Btu/lb, and α = 0.

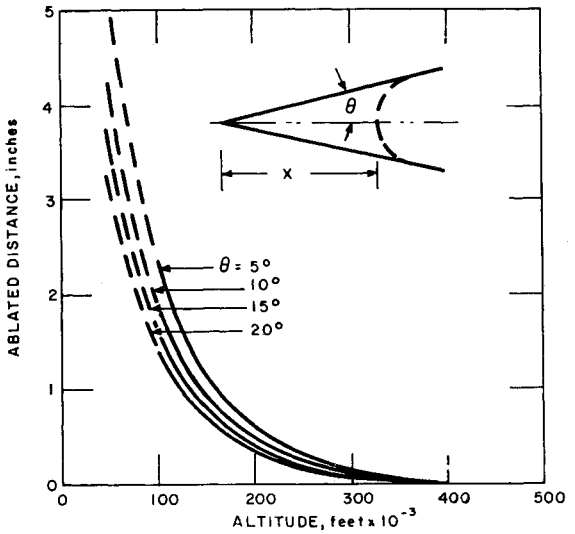

Fig. 16 Ablated distance vs altitude for Teflon; v = 24,000 fps, γ = 20°, h_{eff} = 5000 Btu/lb, and α = 0.

simplified calculations only a completely laminar boundary layer has been assumed. However, it appears likely that a laminar boundary layer would persist in the nose region of the cone down to at least 100,000 ft.

Conclusions

Simple analytical relationships, based on quasi-steady-state ablation, adequately predict the tip recession and nose radius for plastic cones tested in an arc wind tunnel at a $M \cong 5$. The analysis is most conveniently applied to subliming materials, but can be used, with caution, with melting plastics.

The following conclusions were obtained from the cone experiments: 1) pointed cones at $\alpha = 0$ ablated in a symmetrical, predictable manner; 2) Teflon cones at $\alpha = 10°$ had less tip recession and a larger nose radius than corresponding cones at $\alpha = 0$; 3) the effective heats of ablation at the stagnation region of the Teflon, polyethylene, and polyurethane cones agreed with previous results obtained with stable configurations; and 4) the cross-linking of the polymer chain of polyethylene did not produce any noticeable improvement in its ablation characteristics.

By proper choice of material, cone angle, or test conditions, it may be possible to obtain a stable nose configuration, i.e., a nose radius that does not change with ablation time. Estimates of ablated distance and nose radius for an example case of re-entry into the atmosphere on a ballistic trajectory at 24,000 fps indicated that very little material is lost, and the nose radius remains small down to altitudes of at least 100,000 ft.

References

[1] Adams, M. C., Powers, W. E., and Georgiev, S., "An experimental and theoretical study of quartz ablation at the stagnation point," J. Aerospace Sci. **27**, 535–543 (1960).

[2] Bond, C. E., Cordero, J., Curtiss, H., and Henshall, B., "The development of a 10-megawatt multi-arc center and its use in hypersonic reentry vehicle studies," IAS Paper 62-69 (January 1962).

[3] Fay, J. A. and Riddell, F. R., "Theory of stagnation point heat transfer in dissociated air," J. Aeronaut. Sci. **25**, 73–85 (1958).

[4] Ferri, A. and Zakkay, V., "Measurements of stagnation point heat transfer at low Reynolds numbers," J. Aerospace Sci. **29**, 847–850 (1962).

[5] Cheng, H. K., "Hypersonic shock layer theory of the stagnation region at low Reynolds numbers," *Proceedings of the Heat Transfer and Fluid Mechanics Institute* (Stanford University Press, Stanford, Calif., 1961), p. 161.

[6] Lees, L., "Laminar heat transfer over blunt nosed bodies at hypersonic flight speeds," Jet Propulsion **26**, 265 (1956).

[7] Lees, L., *Space Technology* (John Wiley and Sons, Inc., New York, 1959), pp. 12–17.

[8] Allen, H. J. and Eggers, A. J., Jr., "A study of the motion and aerodynamic heating of missiles entering the earth's atmosphere at high supersonic speeds," NACA TN 4047 (October 1957).

[9] Georgiev, S., Hidalgo, H., and Adams, M. C., "On ablating heat shields for satellite recovery," Avco Everett Research Lab. RR 65 (July 1959).

[10] John, R. and Recesso, J., Avco Research and Advanced Development Div., private communication (1962).

[11] Belason, E. and Recesso, J., Avco Research and Advanced Development Div., private communication (1962).

[12] Recesso, J., Avco Research and Advanced Development Div., private communication (1962).